

## Nonlinear Optics with Phase-Controlled Pulses in the Sub-Two-Cycle Regime

U. Morgner,<sup>1</sup> R. Ell,<sup>1</sup> G. Metzler,<sup>1</sup> T. R. Schibli,<sup>1</sup> F. X. Kärtner,<sup>1</sup> J. G. Fujimoto,<sup>2</sup> H. A. Haus,<sup>2</sup> and E. P. Ippen<sup>2</sup>

<sup>1</sup>High Frequency and Quantum Electronics Laboratory, University of Karlsruhe, Engesserstrasse 5, D-76128 Karlsruhe, Germany

<sup>2</sup>Department of Electrical Engineering and Computer Science and Research Laboratory of Electronics, Massachusetts Institute of Technology, Cambridge, Massachusetts 02139

(Received 6 September 2000)

Nonlinear optical effects due to the phase between carrier and envelope are observed with 5 fs pulses from a Kerr-lens mode-locked Ti:sapphire laser. These sub-two-cycle pulses with octave spanning spectra are the shortest pulses ever generated directly from a laser oscillator. Detection of the carrier-envelope phase slip is made possible by simply focusing the short pulses directly from the oscillator into a BBO crystal. As a further example of nonlinear optics with such short pulses, the interference between second- and third-harmonic components is also demonstrated.

DOI: 10.1103/PhysRevLett.86.5462

PACS numbers: 42.65.Ky, 42.25.Bs, 42.65.Re

Recent progress in ultrashort pulse generation with mode-locked lasers has resulted in waveforms with intensity envelopes shorter than two optical cycles. This makes possible new experiments in nonlinear optics that depend on the electric field waveform specifically and not just on the intensity of the pulse [1,2]. Within such a pulse the field oscillation at the optical frequency is not fixed with respect to the pulse envelope but has an additional degree of freedom—the carrier-envelope phase  $\phi$ , defined by the delay between the envelope maximum and the next peak of the carrier oscillation.

The carrier-envelope phase of pulses emerging from a laser is not known *a priori*, and it generally slips from pulse to pulse because the round-trip phase delay in a laser is usually not the same as the round-trip group delay. Nonlinear optical measurements that are sensitive to this carrier-envelope phase are not only interesting in their own right but can have a large impact on metrology as well. The slip rate of this phase determines the absolute positions of the frequency combs produced by mode-locked lasers, and these regularly spaced combs can be used to bridge the gap between atomic clock standards and optical frequencies [3–6].

Very recently, two groups have observed and stabilized the pulse-to-pulse carrier-envelope phase slip  $\Delta\phi$  by spectrally broadening femtosecond laser pulses in an optical fiber [5,7]. Subsequently, the long wavelength part of the pulse spectrum is doubled in a nonlinear crystal and brought to interference with the properly retarded short wavelength part of the pulse spectrum. In this paper, we describe the direct observation of a phase-dependent optical effect occurring in nonlinear media. We report on the determination and stabilization of  $\Delta\phi$  using pulses obtained directly from a mode-locked laser using  $\chi^{(2)}$  and  $\chi^{(3)}$  processes.

The electric field component of a linearly polarized pulse at a given point in space can be decomposed into its analytic parts in different half-planes of the frequency domain [8]

$$E(t) = E^{(+)}(t) + \text{c.c.} = A(t)e^{-i\omega_0 t + i\phi} + \text{c.c.} \quad (1)$$

with the complex field envelope  $A(t)$ , the carrier angular frequency  $\omega_0$ , and the carrier-envelope phase  $\phi$ . It is obvious that such a decomposition into carrier and envelope is not, in general, unique. On the other hand, the pulse intensity  $I(t)$ —and its FWHM—is uniquely related to the absolute square of the analytic signal component  $I(t) \sim |E^{(+)}(t)|^2 = A(t)A^*(t)$  [8].

For special pulses one can choose a carrier frequency and phase, such that the envelope  $A(t)$  becomes real. Only then can the electric field from Eq. (1) be written as  $E(t) = A(t) \cos(\omega_0 t + \phi)$ . If we further define the local time  $t$  such that  $A(t)$  is a maximum at  $t = 0$ , then  $\phi$  measures the deviation of the carrier phase from this maximum.

Of course, such a field is only a freely propagating optical field if it has no dc component. Since  $A(t)$  is real, this also implies that the optical spectrum cannot have components at frequencies above twice the carrier frequency, i.e., for  $|\omega| > 2\omega_0$ . There are other physically plausible fields without the high frequency constraint but then  $\phi$  cannot be independent of time if  $A(t)$  is real. In a qualitative sense, however, a carrier-envelope phase can always be defined near the peak of the pulse.

For all physically realizable fields, the optical power spectrum has to be independent of  $\phi$ , because linear propagation through dispersive media cannot change the power spectrum, even though it changes the carrier-envelope phase by a value  $\Delta\phi_{\text{lin}}$  [9,10]. The carrier propagates with the phase index  $n$ , while the propagation of the pulse envelope is given by the group index  $n_{\text{gr}}$ :

$$\Delta\phi_{\text{lin}} = \frac{2\pi}{\lambda} (n - n_{\text{gr}})L = 2\pi \frac{dn}{d\lambda} L, \quad (2)$$

with the thickness of the medium  $L$ .

The pulse-to-pulse carrier-envelope phase shift  $\Delta\phi$  in a mode-locked laser can easily be changed by varying the intracavity dispersion, i.e., by changing the insertion of a prism or by tilting the prismatic end mirror [11].

Variation of the pulse power may also be used to induce an additional nonlinear phase shift term  $\Delta\phi_{\text{nonlin}}$  [7,9]. Neglecting noise, the carrier-envelope phase evolves with the global time  $T$  in units of the cavity round-trip time according to

$$\phi = \phi_0 + \Delta\phi \frac{T}{T_R} = \phi_0 + (\Delta\phi_{\text{lin}} + \Delta\phi_{\text{nonlin}}) \frac{T}{T_R}.$$

For a pulse repetition rate of  $f_R = 1/T_R$ , the frequency  $f_\phi = \frac{\Delta\phi}{2\pi} f_R$  indicates the rate with which the electric field of the pulse is reproduced in the train of output pulses. The knowledge of  $f_R$  and  $f_\phi$ , which are both in the rf range, defines the absolute positions of frequencies in the mode comb completely [11].

Measurements of intensity, or even of the coherent interference of the pulse with itself, cannot provide information about  $\phi$ . Interferometric cross correlations of successive pulses can reveal pulse-to-pulse slip [9] but do not provide sufficient accuracy for controlling a slow slip. A phase-dependent nonlinear optical measurement is needed. By raising  $E(t)$  in Eq. (1) to the  $n$ th power, it becomes apparent that the  $n$ th power (harmonic) of the pulse field would have a phase offset of  $n\phi$ . The carrier-envelope phase  $\phi$  is thus observable by detecting the interference between optical harmonic components of different orders. The source of such interference is illustrated in Fig. 1 which shows, for example, a rectangularly shaped fundamental spectrum together with the spectra generated from it by instantaneous  $\chi^{(2)}$  (squaring)—and  $\chi^{(3)}$  (tripling)—processes. The necessary spectral span  $[f_1, \dots, f_2]$  for observing an overlap between  $n$ th and  $m$ th harmonic components is determined by the condition

$$f_2 = \frac{m}{n} f_1 \quad (\text{with } f_1 < f_2 \text{ and } n < m). \quad (3)$$

In order to obtain an interference between fundamental and second order at least one octave of spectrum is required. Such an interference was first demonstrated in [5], using a standard Ti:sapphire oscillator with subsequent external spectral broadening in an air-silica microstructure fiber. Second-harmonic components were generated

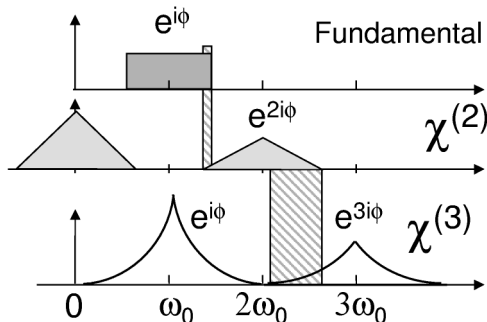


FIG. 1. Schematic spectra of a pulse covering one octave on an optical frequency scale together with the spectra generated by  $\chi^{(2)}$  and  $\chi^{(3)}$  processes, given by successive convolution of the fundamental spectrum.

separately and then recombined with selected fundamental components to observe the interference. A similar result was achieved [7] using only standard fiber with high energy 9-fs pulses produced by a long-cavity Ti:sapphire oscillator. In our work the interference occurs within the femtosecond pulse itself, during propagation of the pulse through the nonlinear crystal. The different frequency components are not separated in time by the dynamics of self-phase modulation and fiber dispersion.

From Eq. (3) it follows that the fundamental bandwidth required to obtain overlap of adjacent harmonics decreases with harmonic order. Thus, these effects can become relevant even with relatively narrow bandwidth pulses in a nonlinear system of higher order. In particular, they may have a large impact on high-harmonic generation, where the generation efficiency can be undermined by the destructive interference between harmonics due to an unfavorable carrier-envelope phase [1,2].

Until recently, spectra obtained directly from a laser have been significantly narrower than one octave [12,13]. For the experiments reported here, octave spanning spectra are made possible by the introduction of double-chirped mirror pairs [14] into a strongly dispersion-managed Kerr-lens mode-locked (KLM) Ti:sapphire laser [15].

The laser setup using these advances is described in detail in [16]. The cavity is designed in a double-Z-folded scheme. A thin Ti:sapphire crystal at one intracavity focus is pumped by a 532-nm laser. A plate of BK7 is placed at the second intracavity focus. The dispersion in the resonator is compensated by double-chirped mirrors and two CaF<sub>2</sub> prisms allow for fine-tuning of the dispersion. With an absorbed pump power of 4 W the cw output power was 30 mW. After the soft-aperture KLM action was initiated by moving a prism, the output power increased to typically 120 mW.

The double-chirped mirror pairs allow for dispersion compensation from 600 to 1200 nm while being highly reflective over the full octave. The pairs are designed so that the dispersion ripple of one mirror cancels that of the second. In the cavity they are used in sequential pairs. With the addition of the second focus and the plate, the choice of a proper dispersion map becomes a key requirement, as shown in [15]. The details of the dispersion map are given in [16].

The optical power spectrum at the laser output is displayed in Fig. 2 on both linear and logarithmic scales. In its wings the spectrum extends over one octave from 600 to 1350 nm. The FWHM of the corresponding pulse assuming a flat phase would be 4.3 fs. The oscillations in the spectrum have their origin in the residual dispersion ripple caused by fabrication tolerances of the mirrors and the transmission properties of the output coupling mirror.

After extracavity dispersion compensation the interferometric autocorrelation measurement (IAC) is obtained by a second-harmonic interferometric autocorrelator. The result is displayed in the inset in Fig. 2. A phase retrieval algorithm [17] is used to reconstruct the IAC completely

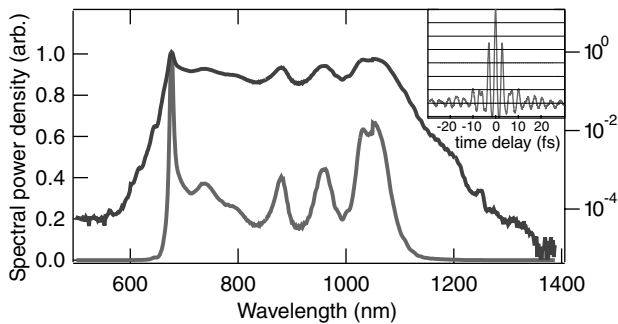


FIG. 2. Output power spectrum on both logarithmic and linear scales. It extends over more than one octave. Inset: Measured IAC of the pulse revealing a pulse width of 5 fs.

from the spectrum. This reconstruction yields a FWHM of 5 fs for the pulse.

The setup for the direct observation of a phase-sensitive nonlinear optical effect is shown schematically in Fig. 3. The signal is enhanced by spectrally selecting and detecting only a narrow portion of the output at the high frequency end of the fundamental pulse spectrum. As indicated above, a phase-dependent signal in this region may be thought of as due to the interference between low frequency second-harmonic components and high frequency fundamental components. But here, these components are not generated separately in space and time. The newly generated components at the second harmonic lead to a distortion of the pulse shape and polarization, so that under proper projection via a polarizer and a filter,

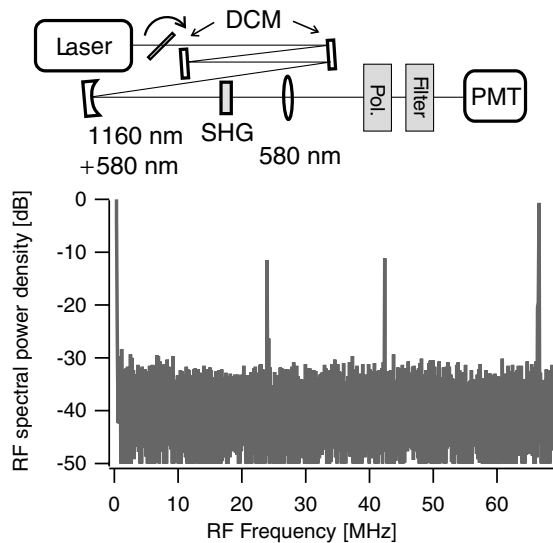


FIG. 3. Top: Experimental setup: Three bounces on double-chirped mirrors (DCM) and a tiltable glass plate allow for tunable group delay compensation. Frequency doubling occurs in a 1-mm thick BBO crystal. A PMT detects the carrier-phase-dependent output behind a 10-nm wide wavelength filter and a polarizer. Bottom: rf spectrum of the PMT signal. The right peak at 65 MHz is from the repetition rate  $f_R$ . The two inner peaks represent the carrier-envelope phase evolution frequency  $f_\phi$  and the mixing product  $f_R - f_\phi$ . The background is from shot noise.

the resulting electric field leads to a significantly phase-dependent detector signal. Note the group delay variations in the crystal over the spectral width of the pulse are about 60 fs. In order to guarantee overlap of the spectral components at 580 nm, the chirp of the input pulse is controlled by three double-chirped mirror reflections and a tiltable 0.5-mm thick glass plate between the laser and the nonlinear crystal. The rf spectrum of this detected signal is displayed in the lower part of Fig. 3. The peak at 65 MHz corresponds to the fundamental repetition rate  $f_R$ . The two peaks in the center, above the shot-noise floor, are the carrier-envelope phase evolution frequency  $f_\phi$  and the mixing product  $f_R - f_\phi$ . The width of the  $f_\phi$  peak is narrower than 10 kHz, and in the free running system  $f_\phi$  changes slowly (on a 100-ms time scale) in a 5-MHz window (see also Fig. 5).

We have also observed the beat between second- and third-harmonic components of the pulse spectrum. In this case, because we do not have a medium with large enough  $\chi^{(2)}$  and  $\chi^{(3)}$  nonlinearities, we optimize the nonlinear interaction by separating the processes as shown in Fig. 4. The pulse train from the laser is launched into a Mach-Zehnder-type interferometer. The short wavelength part of the spectrum around 660 nm is coupled into one arm (arm I), the long wavelength part around 990 nm into arm II. In arm I a 1-mm thick critically phase-matched beta-barium-borate (BBO) crystal produces the second harmonic at 330 nm. In arm II a 0.5-mm thick temperature-tuned, noncritically phase-matched KNbO<sub>4</sub> crystal produces second-harmonic light at 495 nm. To generate the third harmonic in arm II, the fundamental and the second harmonic are summed in a subsequent 1-mm thick critically phase-matched BBO crystal, after proper definition of polarization and temporal overlap.

The beams from the two arms, each with a power of a few nW, are superimposed by a beam splitter. For observation of the signal depending on the carrier-envelope phase,

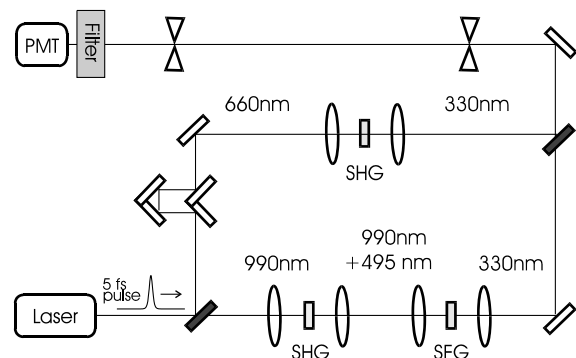


FIG. 4. Interference between second and third harmonic. Top: Setup: In the lower branch of the Mach-Zehnder-type interferometer third harmonic of the long wavelength end of the laser spectrum is generated by two subsequent nonlinear crystals. In the upper branch the second harmonic of the short wavelength end is generated. The beams are superimposed at the upper right beamsplitter (black). A PMT detects the beat frequency behind a spatial and a wavelength filter.

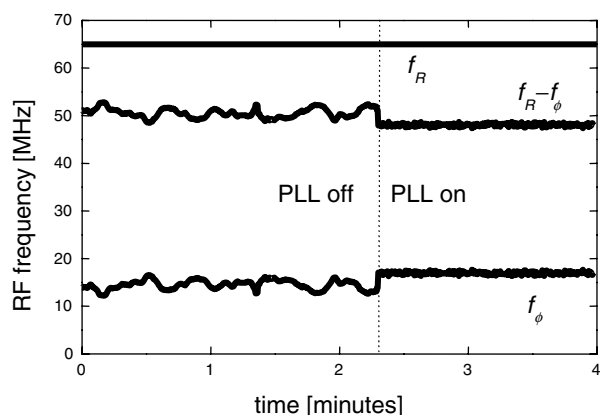


FIG. 5. Stability of the carrier-envelope phase evolution frequency  $f_\phi$  with/without external stabilization to an rf oscillator by means of a phase-locked loop (PLL).

three overlap requirements have to be accomplished: temporal overlap between the two arms—adjusted by the delay line in arm I, spatial overlap between the beams from the two arms—assured by aligning the beams through two pinholes acting as spatial filters, and spectral overlap—selected with a 10-nm wide spectral filter in front of the photomultiplier tube (PMT). The results from this measurement are very similar to those described above for fundamental and second-harmonic interference.

Equation (2) implies that the carrier-envelope phase is affected by a linear and a nonlinear contribution. In contrast to [7,9], we could not observe correlations between amplitude fluctuations of the laser and the position of  $f_\phi$ . In our case, the observed fluctuations of  $f_\phi$  are dominated by environmental noise. The major contribution appears to be a jitter in the intracavity beam pointing angle (in the  $\mu\text{rad}$  range) which translates to dispersion fluctuations at the prisms. Higher stability might be achieved with an acoustically isolated and/or prismless oscillator.

With a phase-locked loop, we then successfully locked the phase-slip frequency to an external rf oscillator, as shown in Fig. 5. The fluctuation spectrum provides a convenient detection window between the time constants of the laser dynamics (in the microsecond range) and the time constants of environmental fluctuations (in the 100-ms range) so that heterodyne locking, using  $f_\phi$  as a reference frequency, is possible with integration times up to 10 ms. In order to guarantee a fixed phase relationship for the emitted pulses, one could either lock the rate to a submultiple of the pulse repetition rate and select constant  $\phi$  pulses at that lower frequency or use a heterodyne locking scheme to lock  $f_\phi$  to zero [5].

In conclusion, we report on two nonlinear optical experiments which reveal the pulse-to-pulse carrier-envelope phase shift of pulses obtained directly from a mode-locked laser. These experiments are made possible by the octave-spanning spectrum of the sub-two-optical cycle pulses that are generated by the laser. No external spectral broadening is required.

The first experiment demonstrates phase-sensitive output by focusing the short pulse into a single nonlinear crystal. The second experiment extends the observation of carrier-envelope phase effects to higher order nonlinearities. In both cases the phase evolution has been successfully locked to an rf oscillator to produce a light source of phase-controlled sub-two-cycle pulses that can enable further progress in phase-dependent nonlinear optics as well as in metrology.

U. Morgner and F.X. Kärtner acknowledge support from the Deutsche Forschungsgemeinschaft (DFG). This research was supported by the Air Force Office of Scientific Research Contract No. F4920-98-1-0139 and the Medical Free Electron Laser Program, Office of Naval Research Contract No. N00014-94-1-0717.

- [1] T. Brabec and F. Frausz, *Rev. Mod. Phys.* **72**, 545–591 (2000).
- [2] C. Durfee, A. Rundquist, S. Backus, C. Herne, M. Murnane, and H. Kapteyn, *Phys. Rev. Lett.* **83**, 2187 (1999).
- [3] T. Udem, J. Reichert, R. Holzwarth, and T. Hänsch, *Phys. Rev. Lett.* **82**, 3568 (1999).
- [4] J. Reichert, M. Niering, R. Holzwarth, M. Weitz, T. Udem, and T. Hänsch, *Phys. Rev. Lett.* **84**, 3232 (2000).
- [5] D. Jones, S. Diddams, J. Ranka, A. Stentz, R. Windeler, J. Hall, and S. Cundiff, *Science* **288**, 635 (2000).
- [6] M. Bellini and T. Hänsch, *Opt. Lett.* **25**, 1049 (2000).
- [7] A. Apolonski, A. Poppe, G. Tempea, C. Spielmann, T. Udem, R. Holzwarth, T. Hänsch, and F. Krausz, *Phys. Rev. Lett.* **85**, 740 (2000).
- [8] D. Gabor, *J. Inst. Electr. Eng. (London)* **93**, 429 (1946).
- [9] L. Xu, C. Spielmann, A. Poppe, T. Brabec, F. Krausz, and T. Hänsch, *Opt. Lett.* **21**, 2008–2010 (1996).
- [10] H. Telle, G. Steinmeyer, A. Dunlop, J. Stenger, D. Sutter, and U. Keller, *Appl. Phys. B* **69**, 327–332 (1999).
- [11] J. Reichert, R. Holzwarth, T. Udem, and T. Hänsch, *Opt. Commun.* **172**, 59–68 (1999).
- [12] U. Morgner, F. Kärtner, J. Fujimoto, E. Ippen, V. Scheuer, G. Angelow, and T. Tschudi, *Opt. Lett.* **24**, 411–413 (1999).
- [13] D. Sutter, G. Steinmeyer, L. Gallmann, N. Matuschek, F. Morier-Genoud, U. Keller, V. Scheuer, M. Tilsch, and T. Tschudi, *Opt. Lett.* **24**, 631–633 (1999).
- [14] F.X. Kärtner, U. Morgner, R. Ell, T. Schibli, J.G. Fujimoto, E.P. Ippen, V. Scheuer, G. Angelow, and T. Tschudi, *Ultrafast Phenomena* (Springer, Berlin, 2000), Vol. XI, pp. 51–55.
- [15] Y. Chen, F. Kärtner, U. Morgner, S. Cho, H. Haus, E. Ippen, and J. Fujimoto, *J. Opt. Soc. Am.* **16**, 1999–2004 (1999).
- [16] R. Ell, U. Morgner, F.X. Kärtner, J.G. Fujimoto, E.P. Ippen, V. Scheuer, G. Angelow, T. Tschudi, M.J. Lederer, A. Boiko, and B. Luther-Davies, *Opt. Lett.* **26**, 373 (2001).
- [17] A. Baltuska, A. Pugzlys, M. Pshenichnikov, D. Wiersma, B. Hoenders, and H. Ferwerda, in *Proceedings of Ultrafast Optics 1999, Ascona, Switzerland*, edited by François Salin and Ursula Keller (Springer, Berlin, 2000), p. 221.